

Synthesis of Nano Particles

1. Spheroids, Clusters and Spheroidal Holoids

Insulators: Halides, Oxides, Nitrides

Hard/Strong Matter: Carbons, BN, etc.

Semiconductors: Chalcogenides

Metals: Noble Metals, Magnetic Metals

Organic Matter: Polymers, Biopolymers

2. Anisotropic Particles

Insulators: Halides, Oxides, Nitrides

Hard/Strong Matter: Carbons, BN, etc.

Semiconductors: Chalcogenides

Metals: Noble Metals, Magnetic Metals

Organic Matter: Polymers, Biopolymers

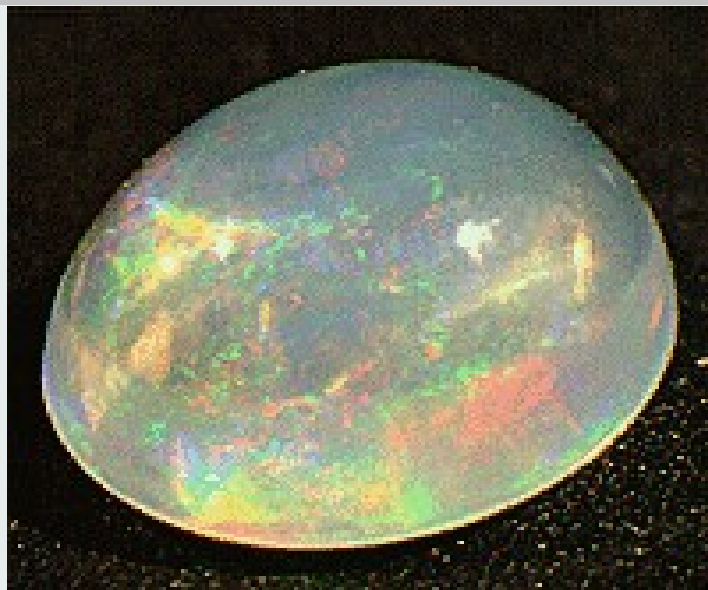
02.11.2006

Nanochemistry UIO

1

Synthesis Routes - Spheroids

1. Natural (Opal)
2. Sol-Gel
3. Solvothermal
4. Templated
5. Hydrolysis
6. Extraction
7. Flame&Gas Phase
8. Phase Transitions
9. Corrosion
10. Block Structures
11. Intercalations

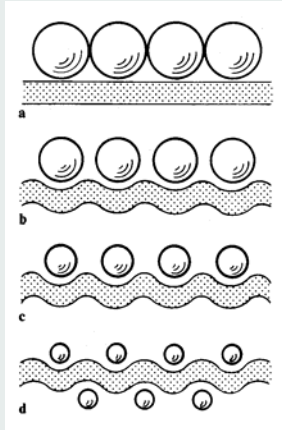
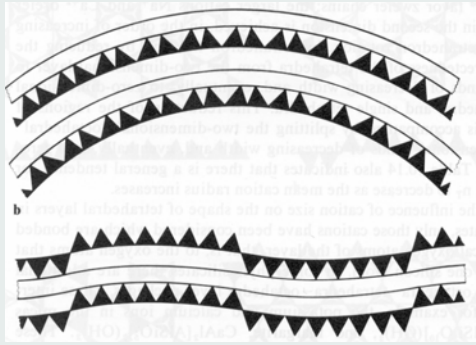


02.11.2006

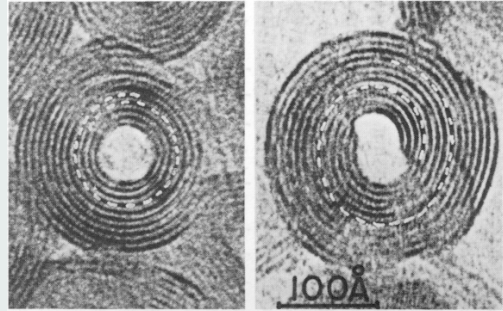
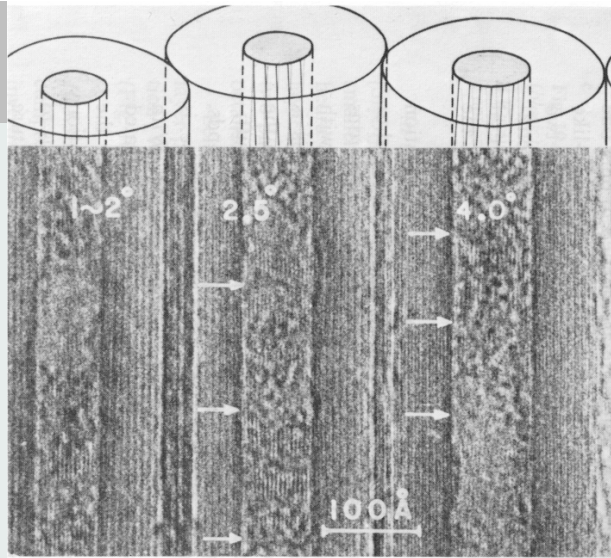
Nanochemistry UIO

2

Bending of a layer



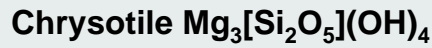
02.11.2006



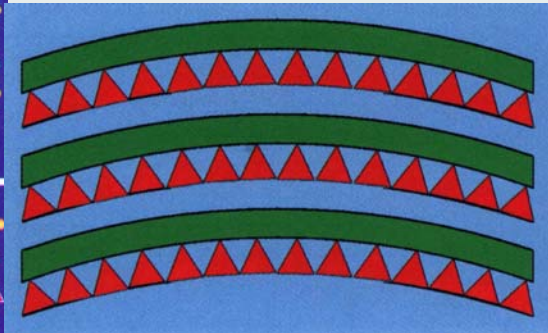
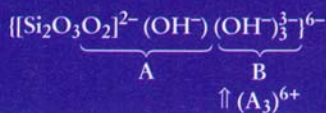
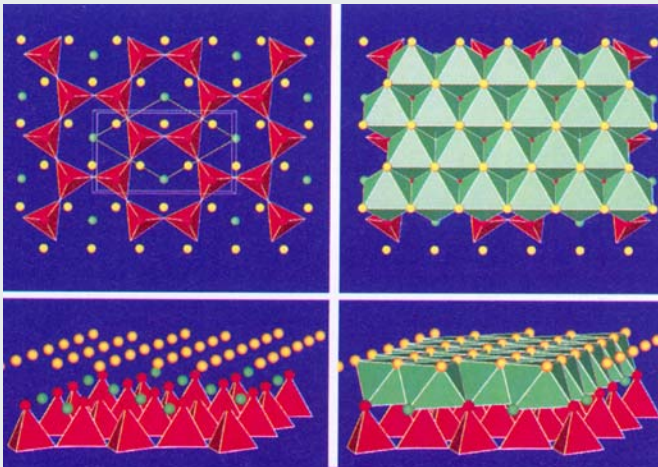
Nanochemistry UIO

3

Single Layer Misfits - Silicate Minerals



Anisotropic structure inside layers causes bending of the double layers



Structure models reproduced from: Röhr, *ChiuZ* 32 (1988) 64

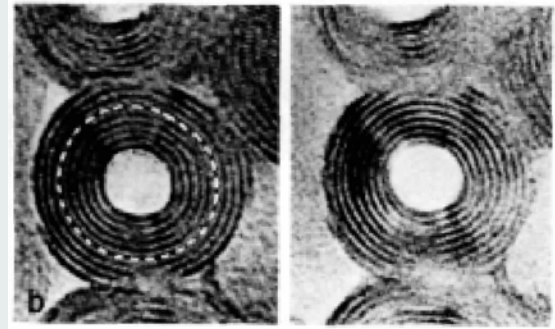
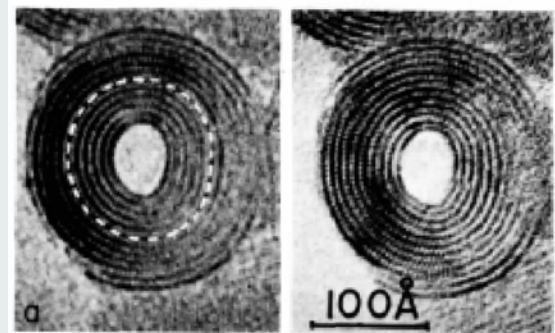
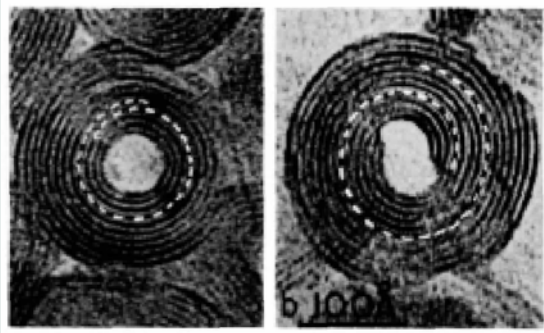
02.11.2006

Nanochemistry UIO

4

Tubular Silicate Minerals

TEM investigation of the cross-sections of Chrysotile

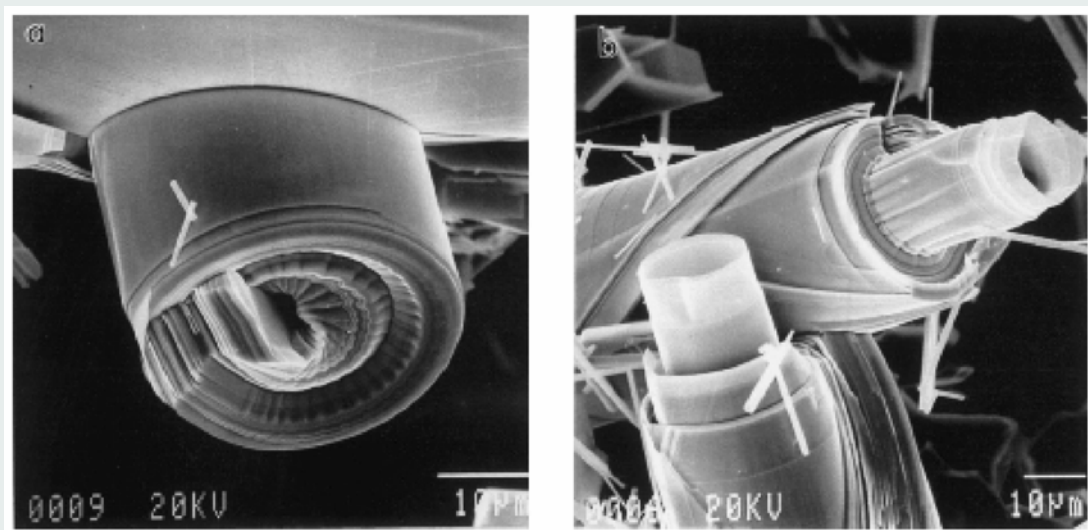


Scrolls of one or more layers

But: also closed, concentric cylinders

Yada, *Acta Crystallogr. A* 27 (1971) 659

Misfit Layer Structures in Ternary Chalcogenides



SEM images of tubular crystals in the system Bi-Nb-S

Landa-Cánovas, Gómez-Herrero, Otero-Díaz, *Micron* 32 (2001) 491

Starting from Solids

1. Topotactic reactions
2. Surface reactions
3. Phase widths
4. Intercalations & Ionic exchange

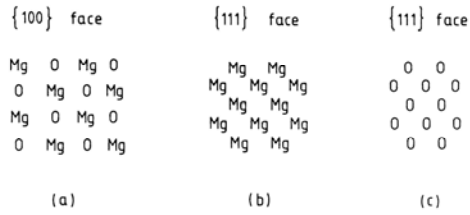
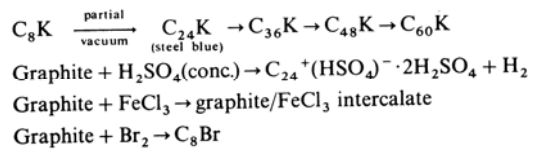
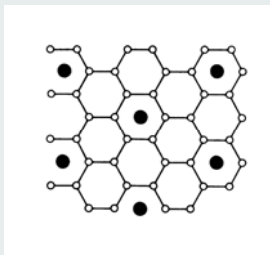
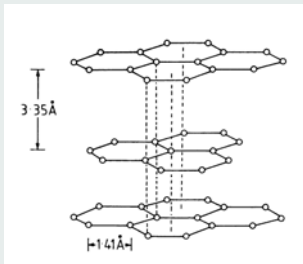


Fig. 2.3 Surface structures of a MgO crystal displaying (a) (100) and (b, c) (111) faces



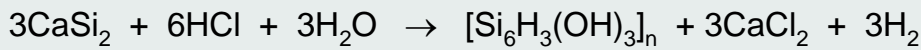
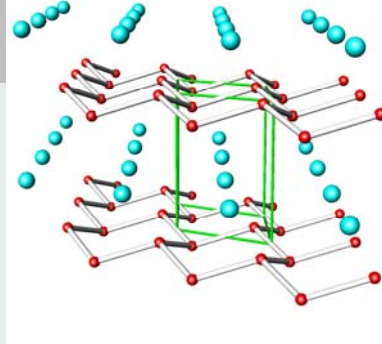
02.11.2006

Nanochemistry UIO

7

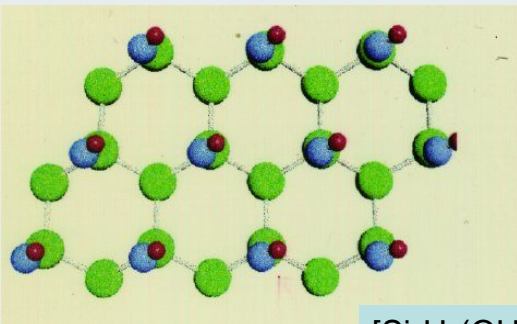
Topochemical Reactions

Siloxenes

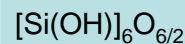
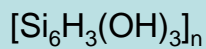
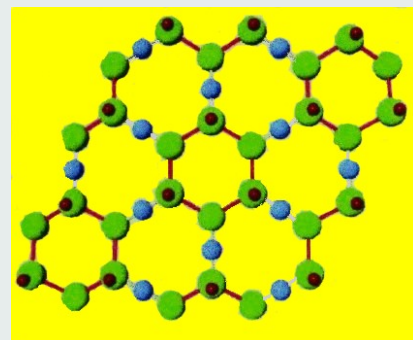


Wöhler 1863

Kautzky 1924



2D-poly
[1,3,5-tri
hydroxy
cyclohexa
silan]



02.11.2006

Nanochemistry UIO

8

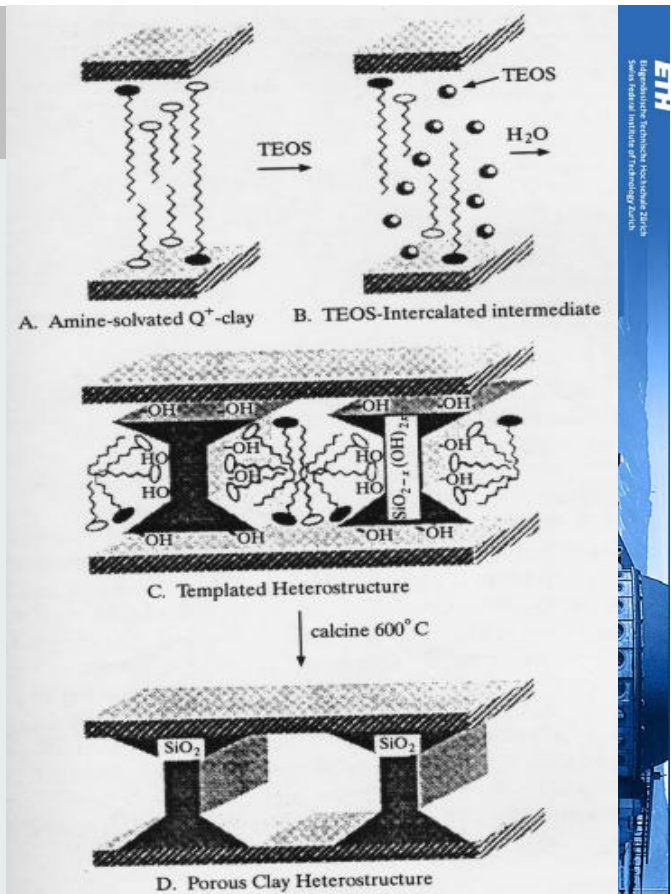
"Das Silicon (= Siloxen) ist lebhaft orange-gelb; es besteht aus durchscheinenden gelben Blättchen[...]. Es ist unlöslich in Wasser, in Alkohol, in Kieselchlorid, in Phosphorchlorid, in Schwefelkohlenstoff. Beim Erwärmen wird es vorübergehend tiefer orange-gelb. Stärker erhitzt entzündet es sich und verbrennt mit schwacher Verpuffung und Funkensprühen unter Zurücklassung von Kieselsäure, die durch amorphes Silicium braun gefärbt ist. Ohne Luftzutritt erhitzt, entwickelt es Wasserstoffgas und hinterläßt ein Gemenge von Kieselsäure und amorphem Silicium in Gestalt glänzender, schwarzbrauner Blättchen. Erst nach vollem Glühen hört die Wasserstoffentwicklung auf. War es mit einer nicht ganz konzentrierten Säure bereitet, so enthält es die weiter unten beschriebene Verbindung beigemischt; es ist dann heller an Farbe und zeigt beim Erhitzen auch in einer Röhre eine Art Verpuffung, unter gleichzeitiger Entwicklung von selbstentzündlichen Kieselwasserstoffgas. Diese Zersetzung des Silicons in der Wärme beginnt schon bei 100 °C[...]."

Sehr merkwürdig ist sein Verhalten im Licht. Im Dunkeln bleibt es, selbst im feuchten Zustand, ganz unverändert; im zerstreuten Licht wird es zunehmend blässer und im direkten Sonnenlicht wird es nach kurzer Zeit vollkommen weiß, und zwar unter Entwicklung von Wasserstoffgas. Stellt man es unter Wasser in den Sonnenschein, so fängt es augenblicklich an Wasserstoffgas zu entwickeln, was gleich einer Gährungserscheinung fort dauert, bis es ganz weiß geworden ist [...]. Das Silicon wird weder von Chlor noch rauchender Salpetersäure oder von konzentrierte Schwefelsäure angegriffen, selbst nicht beim Erhitzen damit. Flußsäure erhitzt sich damit; es erhebt sich darin zugleich an die Oberfläche, wird allmählich heller, zuletzt weiß und verschwindet endlich ganz [...]."

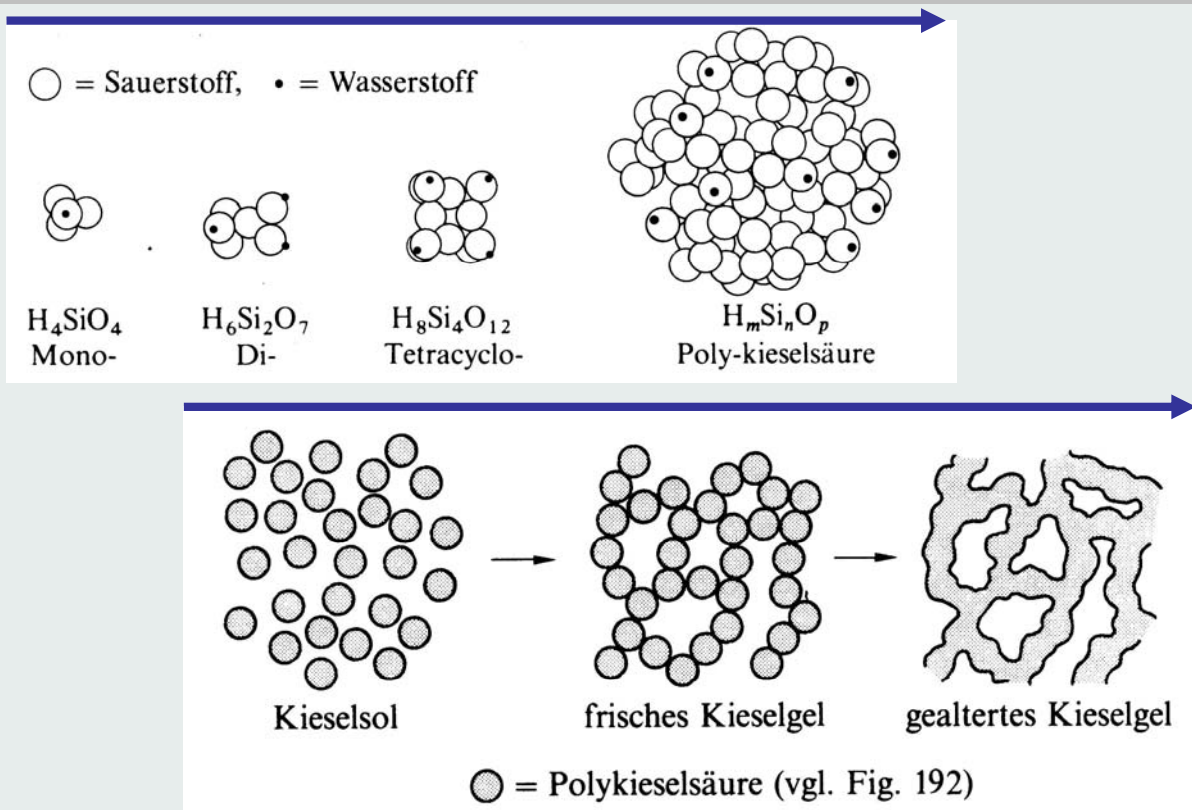
Re-detected ~ 1989 !

Intercalation and Delamination

Layered Materials



Sol-Gel- Route

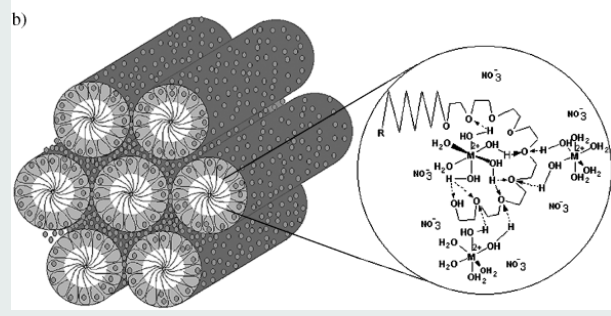
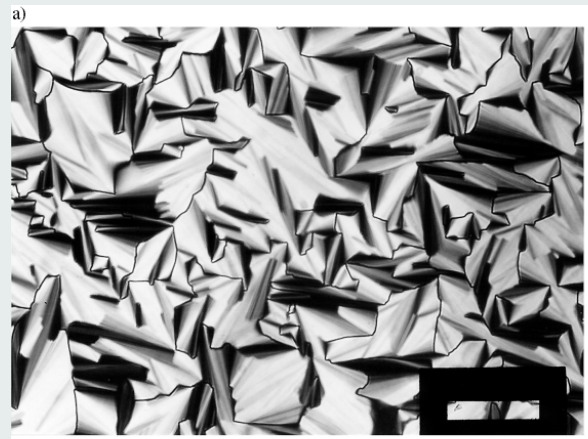
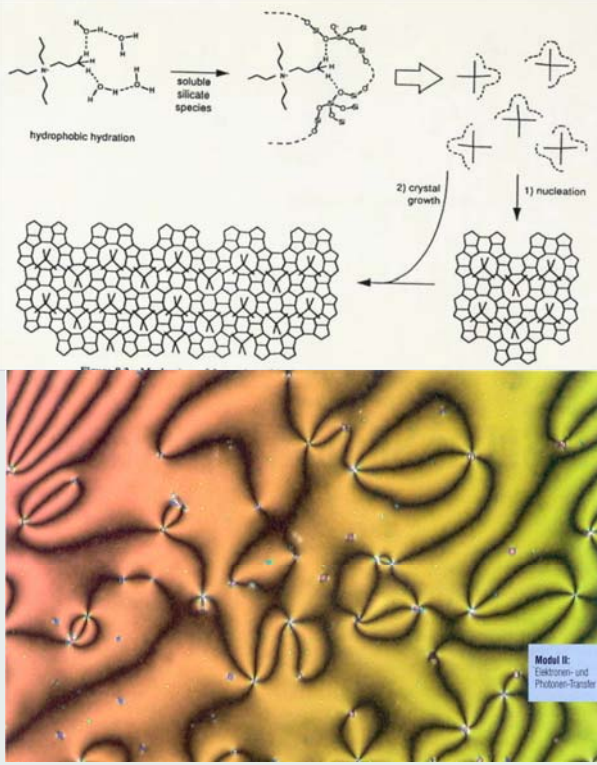


02.11.2006

Nanochemistry UIO

11

Sol-Gel – Templates as Space Holders and Structure Directors



02.11.2006

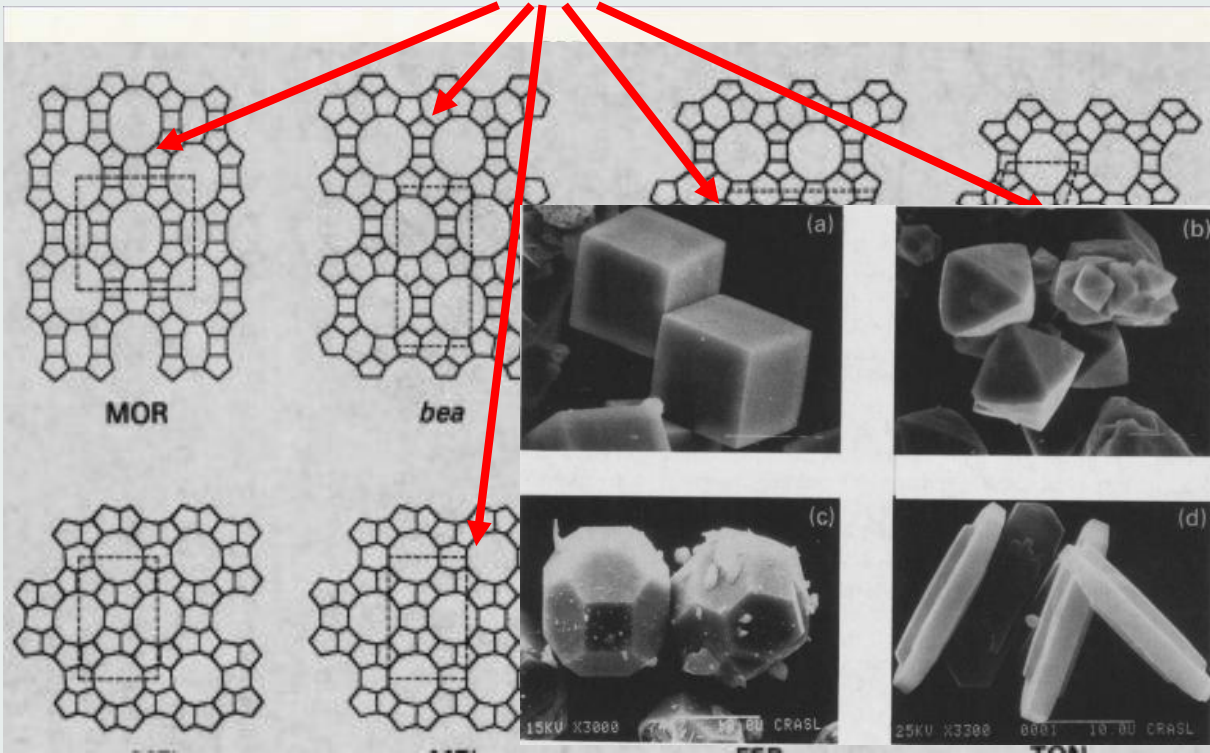
Nanochemistry UIO

12

Zeolites (boiling stones)

concentrations + template + temperature + time + ??

R. NESPER ETH ZÜRICH & COLLEGIUM HELVETICUM



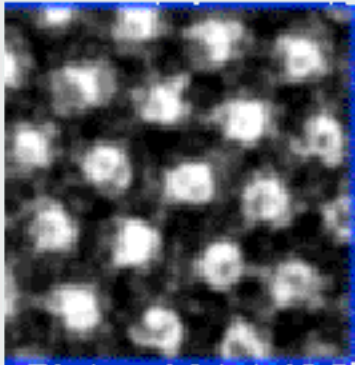
02.11.2006

Nanochemistry UIO

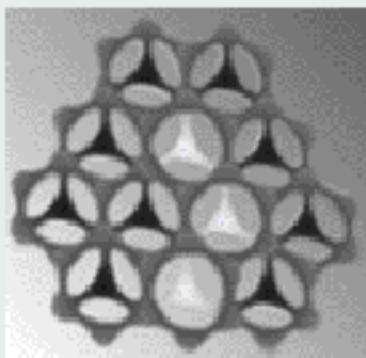
13



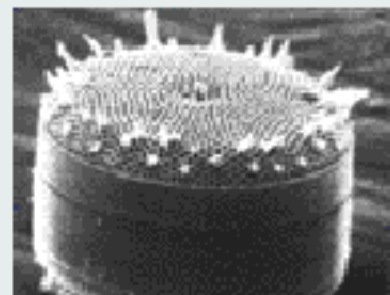
Mesoporous Materials



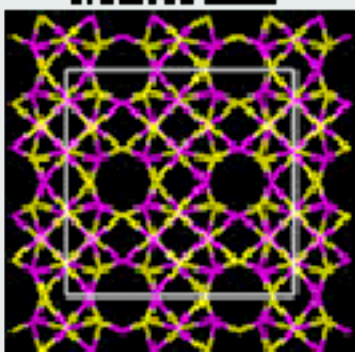
Mesocellular Foams



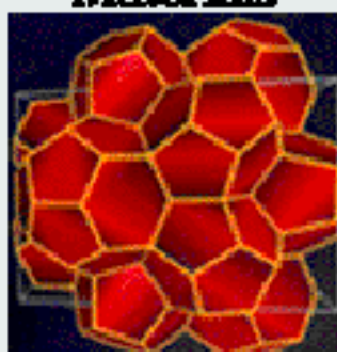
Biomineralization of Silica



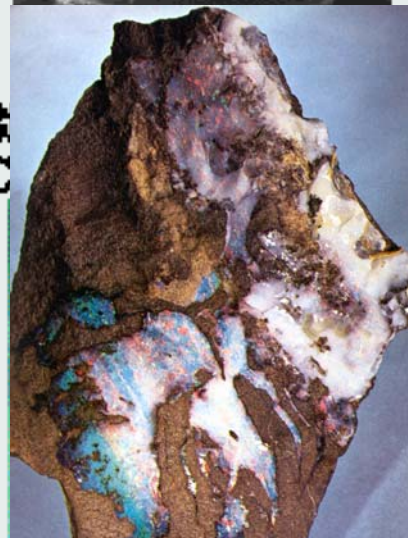
Microporous Materials



Thermoelectric Materials



Bio



R. NESPER ETH ZÜRICH & COLLEGIUM HELVETICUM

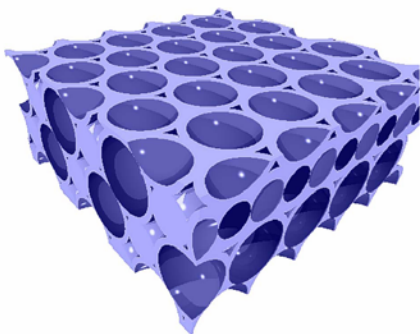


Opals and Photonic Crystals

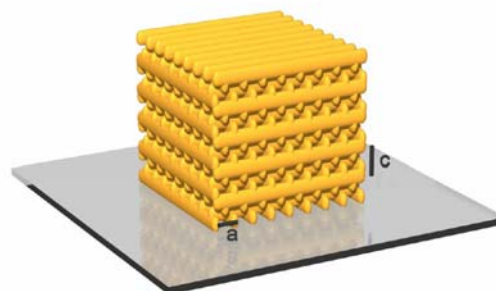
- (styrene) nanobeads + TEOS \rightarrow SiO₂ coated beads
- thermalize beads



3D Photonic Crystals - the **inverse opal**



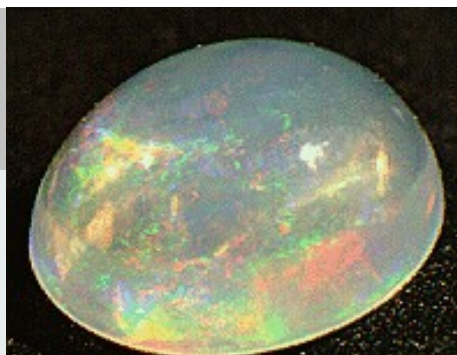
3D Photonic Crystals - the **Woodpile (Layer-by-Layer structure)**



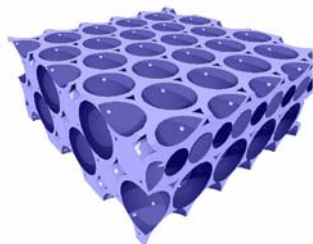
fcc for $(c/a)^2=2$, full gap for index contrast > 1.9 , 25% gap for holes in Si

Opals and Photonic Crystals

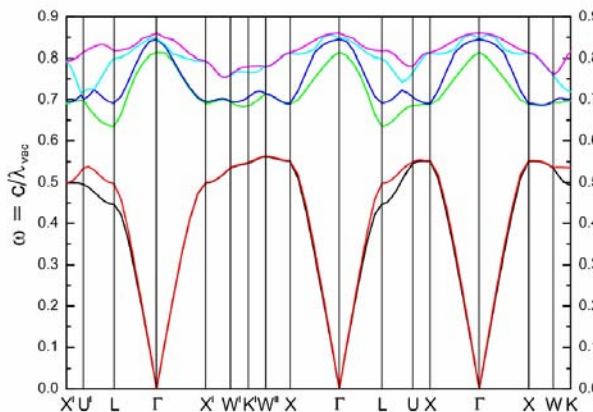
- (styrene) nanobeads + TEOS \rightarrow SiO₂ coated beads
- thermalize beads



3D Photonic Crystals - the **inverse opal**



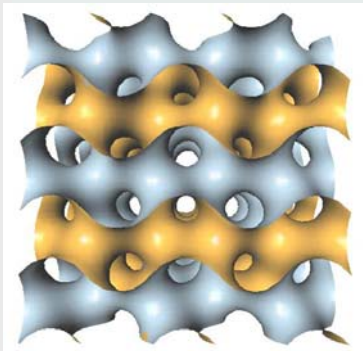
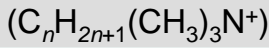
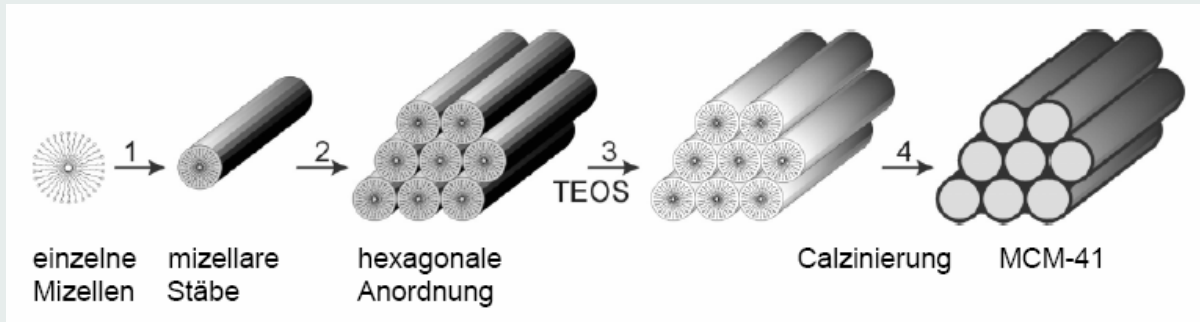
3D Photonic Crystals - the **Woodpile (Layer-by-Layer structure)**



Band structure of a woodpile composed of Si-rods

Proposal: C.M. Soukoulis et al., Solid State Commun. 89, 413 (1994)

Mesoporous Silicates: MCM41 / MCM48

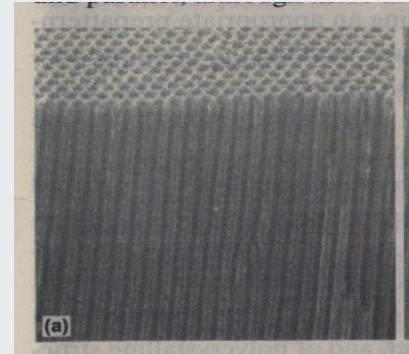


02.11.2006

Tetraethoxysilan, TEOS

MCM 41 – hexagonal Porengrößen 3-8nm

MCM 48 – cubisch 3D-Kanalstruktur



Nanochemistry UIO

17

Ionic Liquids

Characteristic properties:

- low vapour pressure
- thermischal stability
- elektric conductivity
- Phasenseparation from products
- high thermal capacity
- non burning

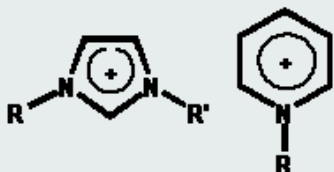
These liquids are – in contrast to salt melts – not corrosive and thus are used to replace ordinary organic solvents

fields of applications

- head carrier
- Elektrolyte
- Analytics
- separator
- Membran etequines

P. Wasserscheid und W. Keim.
Angew. Chem. 2000, 112, 3926-3945.

Kationen und Anionen ir Ionischen Flüssigkeiten: Ausgewählte Beispiele



Cl⁻ BF₄⁻ Br⁻ AlCl₄⁻
PF₆⁻ SbF₆⁻ CF₃SO₃⁻



02.11.2006

Nanochemistry UIO

18

Controlled Precursor Hydrolysis

Polyolate-Route

(ionic liquids)

Cu_2O	ZnO	Mn_3O_4	Al_2O_3	SiO_2	V_2O_5	MoO_3
	CdO		Bi_2O_3	SnO_2	Nb_2O_5	WO_3
	CoO		Y_2O_3	CeO_2	Ta_2O_5	
			La_2O_3	TiO_2		
			Cr_2O_3	ZrO_2		
			Fe_2O_3			
	Zn_2SiO_4	$CaTiO_3$	YVO_4	$MgAl_2O_4$	$ZnNb_2O_6$	
			$MnWO_4$	$BaAl_2O_4$		
				$CoAl_2O_4$		
				$ZnCo_2O_4$		

(als Ausgangsverbindungen wurden verwendet: $Al(sec-OC_4H_9)_3$, $Al(OC_3H_7)_3$, $Ba(CH_3COO)_2$, $Bi(CH_3COO)_3$, $Ca(CH_3COO)_2 \cdot xH_2O$, $Cd(CH_3COO)_2 \cdot xH_2O$, $Ce(CH_3COO)_3 \cdot xH_2O$, $Co(CH_3COO)_2 \cdot 4H_2O$, $CrCl_3 \cdot 6H_2O$, $Cu(CH_3COO)_2 \cdot H_2O$, $Fe(CH_3COO)_2$, $La(CH_3COO)_3 \cdot xH_2O$, $Mg(CH_3COO)_2 \cdot 4H_2O$, $Mn(CH_3COO)_2 \cdot 4H_2O$, $Mo(i-OC_3H_7)_5$, $Nb(OC_2H_5)_5$, $Si(OC_2H_5)_4$, $Sn(C_2H_5)_4$, $Ta(OC_2H_5)_5$, $Ti(OC_2H_5)_4$, $VO(i-OC_3H_7)_3$, $W(OC_2H_5)_5$, $Y_3O(i-OC_3H_7)_{13}$, $Y(i-OC_3H_7)_3$, $Zn(CH_3COO)_2 \cdot 2H_2O$, $Zr(OC_4H_9)_4$)

nanoskalem $VO(i-OC_3H_7)_3$			Reaktions-	Reaktions-	mittlerer Partikel-
$VO(i-OC_3H_7)_3$	H_2O	DEG	temperatur [°C]	dauer [h]	durchmesser [nm]
0,5	1	50	180	1	30 bis 40
2,3	2	50	180	2	60 bis 70
5,5	2	50	180	2	90 bis 100
10,6	2	50	190	8	160 bis 180



02.11.2006

Nanochemistry UIO

19

Controlled Precursor Hydrolysis

Polyolate-Route – Particle Size Distribution

Solvent: DEG (Et(OH)₂) Metal source : Alkoxides, Halides, T ~ 200 °C

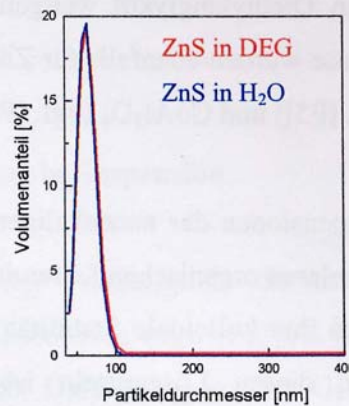
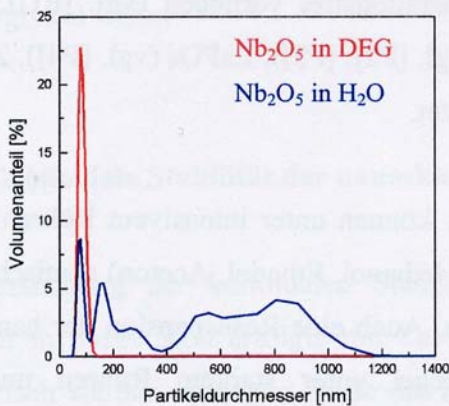


Abb. 4: Partikelgrößenverteilung von nanoskaligem Nb_2O_5 und ZnS in Diethylenglykol sowie nach dem Mischen der DEG-Suspensionen mit Wasser

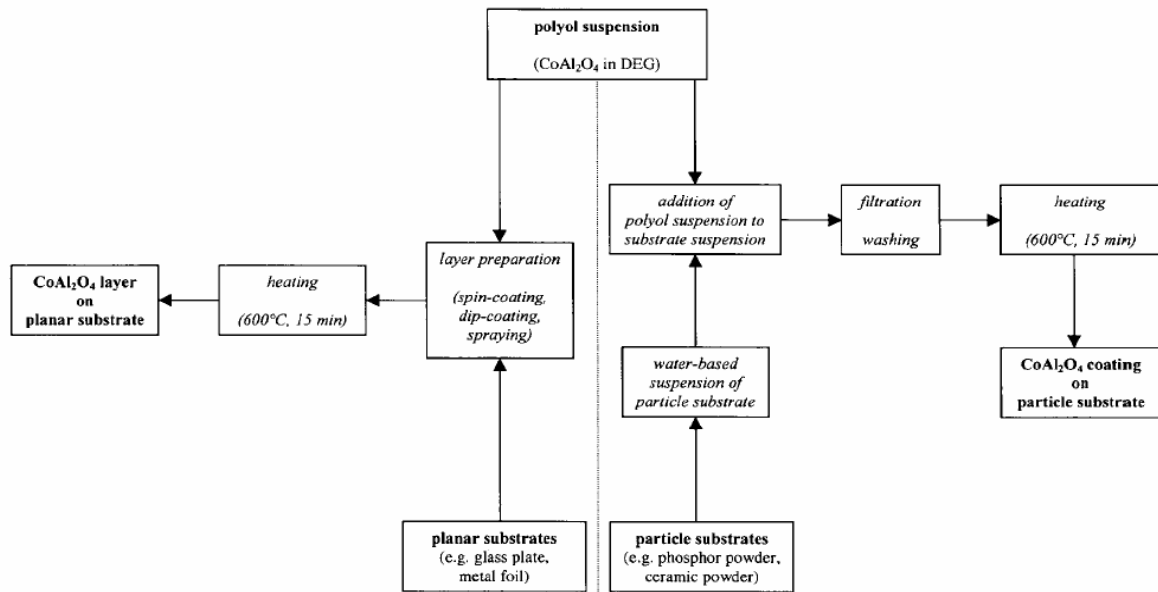
02.11.2006

Nanochemistry UIO

20

Polyolate Route – Magnetic Particles – Coating Recipe

Co(CH ₃ COO) ₂ ·4H ₂ O/g	Al(CH ₃ COO) ₂ OH/g	H ₂ O/ml	DEG/ml	d ₅₀ /nm
0.50	0.72	1	50	56
2.00	2.86	1	50	96
2.00	2.86	3	50	143



02.11.2006

Nanochemistry UIO

21

Controlled Precursor Hydrolysis

Metal Organic Precursors

Room-Temperature Organometallic Synthesis of Soluble and Crystalline ZnO Nanoparticles of Controlled Size and Shape

Miguel Monge, Myrtil L. Kahn, André Maisonnat, and Bruno Chaudret*

Angew. Chem. 2003, 115, 5479–5482

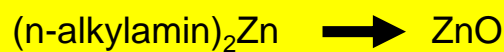
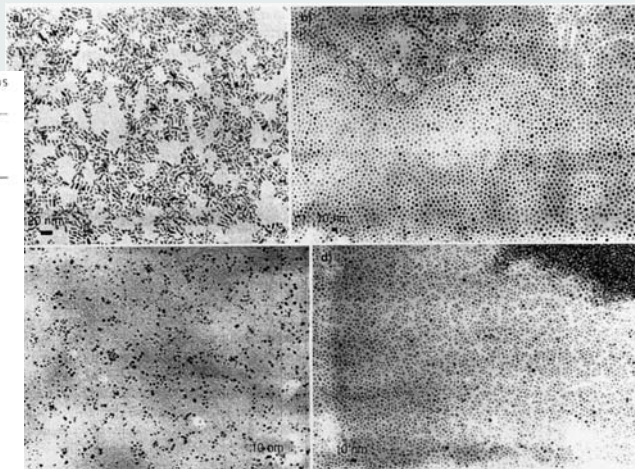


Table 1: Summary of the results obtained after oxidation of the [Zn(C₂H₅)₂] precursor under various reaction conditions.

Ligand added	Solvent	Time	Overall concentration [M]	Temperature	Size [nm] ^[a]	Morphology
–	THF	Standard ^[b]	0.042	RT	–	Agglomerated nanoparticles
HDA	THF	Standard	0.042	RT	8.1 ± 3.3 × 2.6 ± 0.4	Nanorods
HDA	THF	Standard	0.125	RT	11.4 ± 5.7 × 2.8 ± 0.7	Nanorods
HDA	THF	2 weeks	0.042	RT	4.1 ± 0.9	Nanodisks
HDA	THF	Standard	0.042	45 °C	4.8 ± 0.3	Nanodisks
HDA	THF	Standard	0.01	RT	< 3.0 after 1 day 4.3 ± 0.5 after 4 days	Nanodisks
HDA	THF	5 min under Ar	0.042	RT	5.8 ± 1.3 × 2.7 ± 0.3	Nanorods
DDA	THF	Standard	0.042	RT	3.0 ± 0.5	Nanodisks
OA	THF	Standard	0.042	RT	4.0 ± 0.7	Nanodisks
HDA	Toluene	Standard	0.042	RT	4.6 ± 0.9	Nanodisks
HDA	Heptane	Standard	0.042	RT	2.4 ± 0.5	Nanodisks
HDA	–	Standard	–	RT	10.7 ± 1.2 × 1.6 ± 0.3	Nanorods
DDA	–	Standard	–	RT	9.2 ± 2.0 × 3.7 ± 1.8	Nanorods
OA	–	Standard	–	RT	7.4 ± 1.4 × 2.8 ± 0.6	Nanorods
2 HDA	–	Standard	–	RT	–5	Not homogeneous
2 DDA	–	Standard	–	RT	17.1 ± 3.4 × 3.0 ± 0.4	Nanorods
2 OA	–	Standard	–	RT	36.9 ± 10.8 × 2.8 ± 0.3	Nanorods

[a] Standard reaction time is 17 h under Ar and 1 or 2 days of oxidation/evaporation. [b] The values indicate the diameter of nanodisks or the length and width for nanorods; size dispersion is given after the mean size.



02.11.2006

Nanochemistry UIO

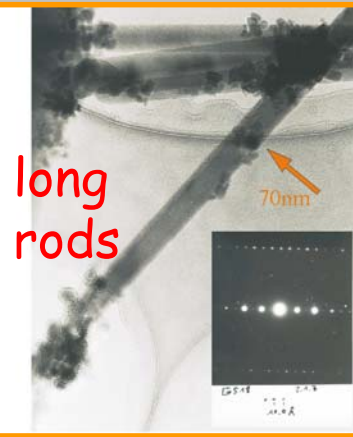
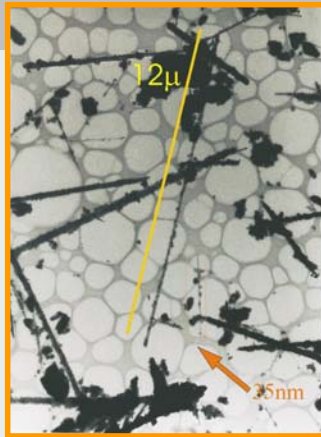
22

Alkoxide Hydrolysis

R. NESPER, ETH ZÜRICH & COLLEGIUM HELVETICUM



small needles



long rods

FeO_x NPs

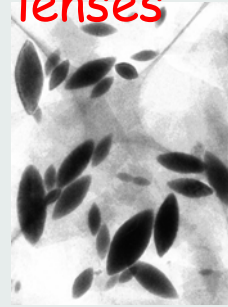


small rods



large needles

small lenses



large cubes

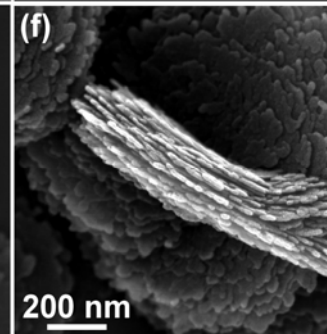
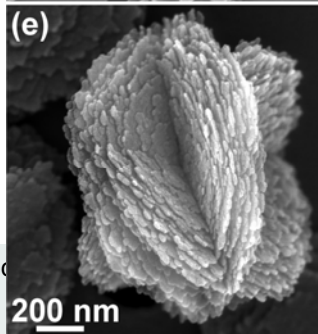
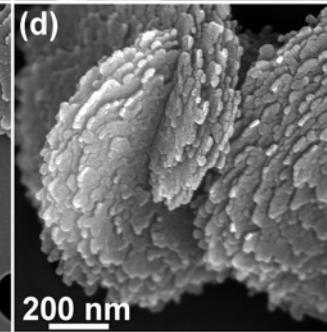
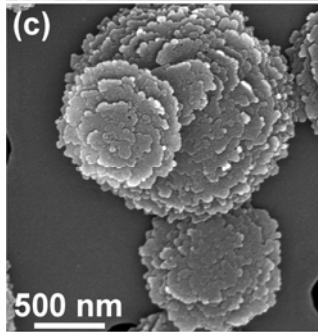
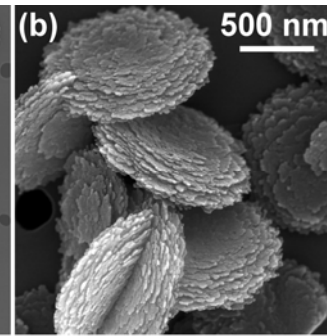
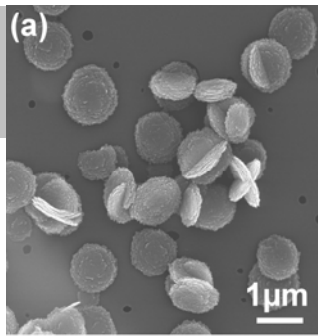
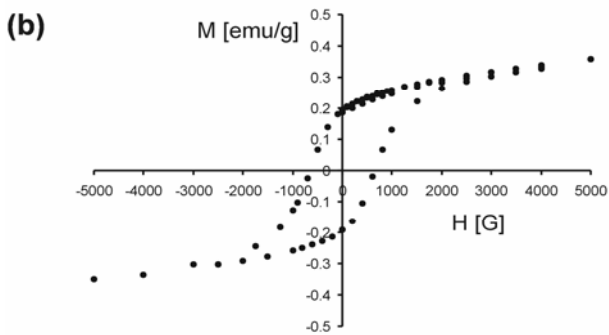
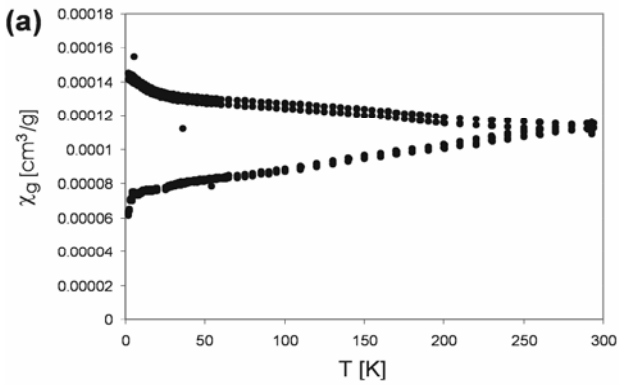


02.11.2006

Nanochemistry UIO

23

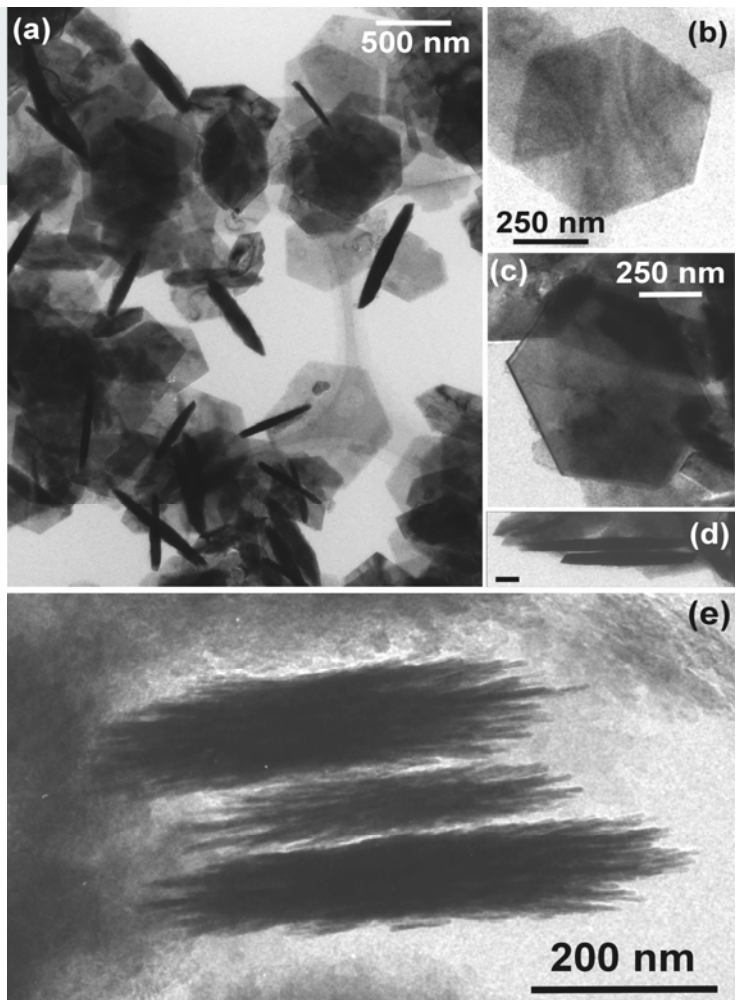
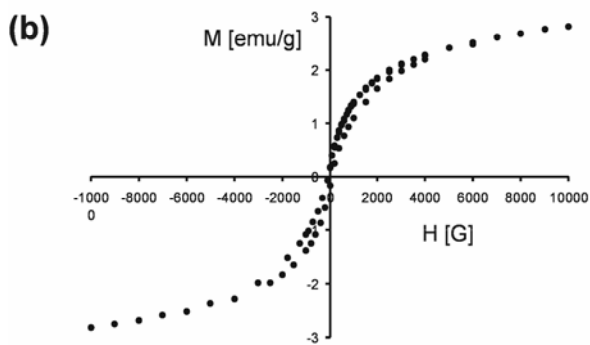
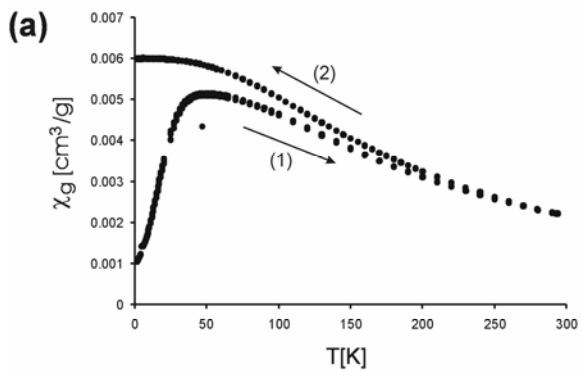
Hematite-Discs



02.11.2006

Nano

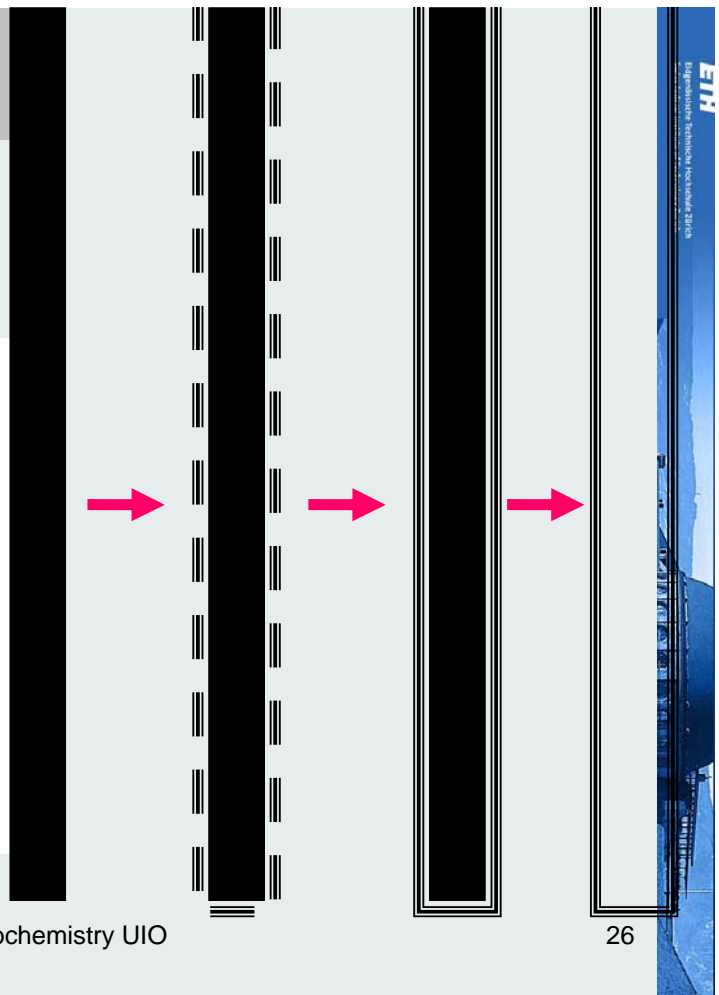
Hematite-Discs



Secondary Nanoparticles

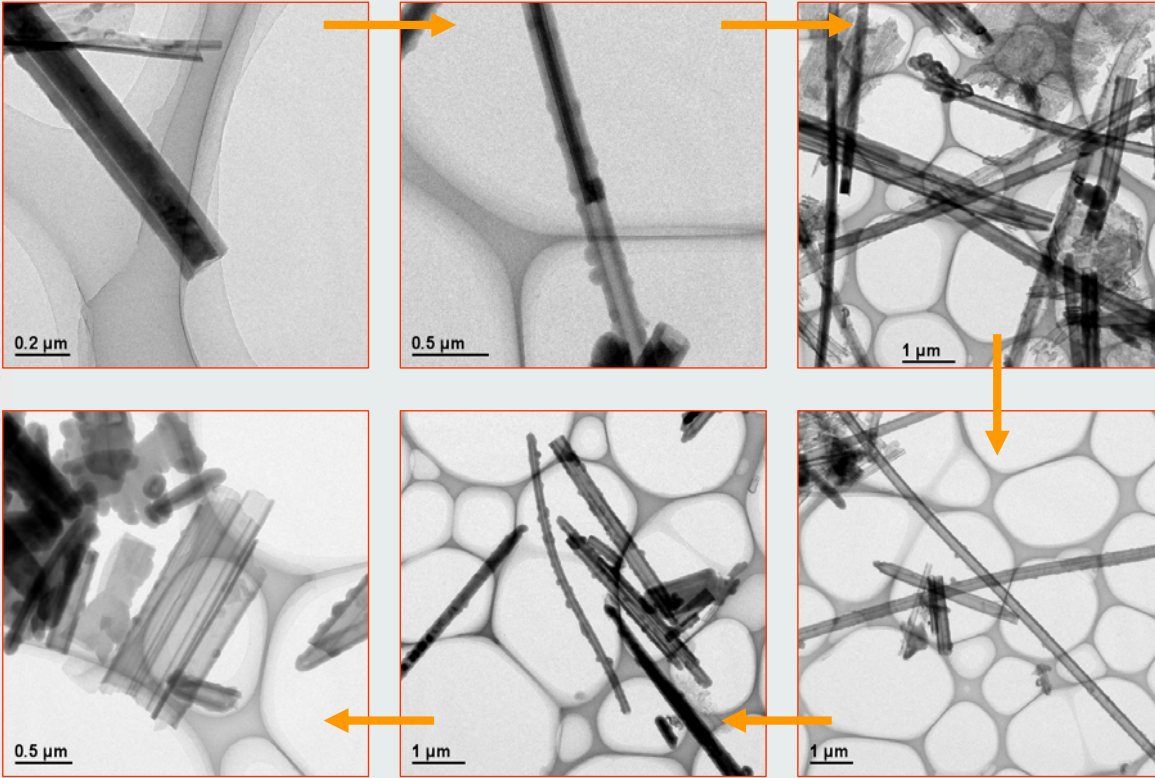
R. NESPER ETH ZÜRICH & COLLEGIUM HELVETICUM

1. V_2O_5 nanofibers
2. Coating utilizing TEOS
3. Calcination
4. Emptying
5. SiO_2 secondary nanotubes



Nanotubular SiO₂

R. NESPER, ETH ZÜRICH & COLLEGIUM HELVETICUM



02.11.2006

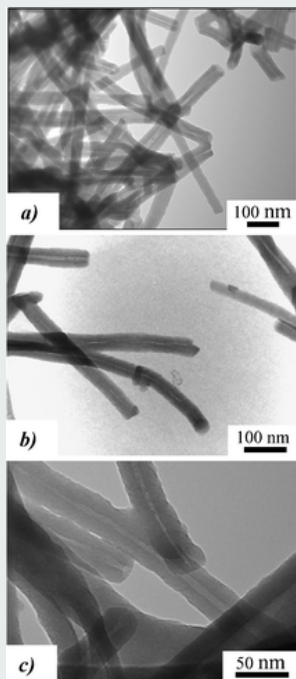
Nanochemistry UIO

27

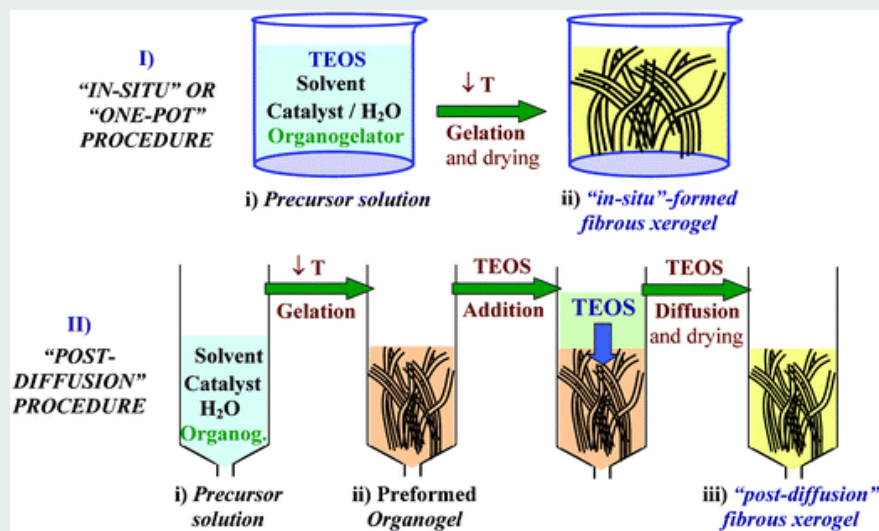
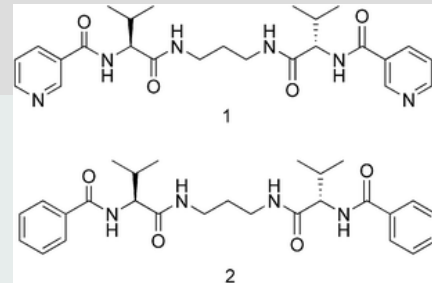


Applying Organogels

J. Mater. Chem., 2006,



02.11.2006



Nanochemistry UIO

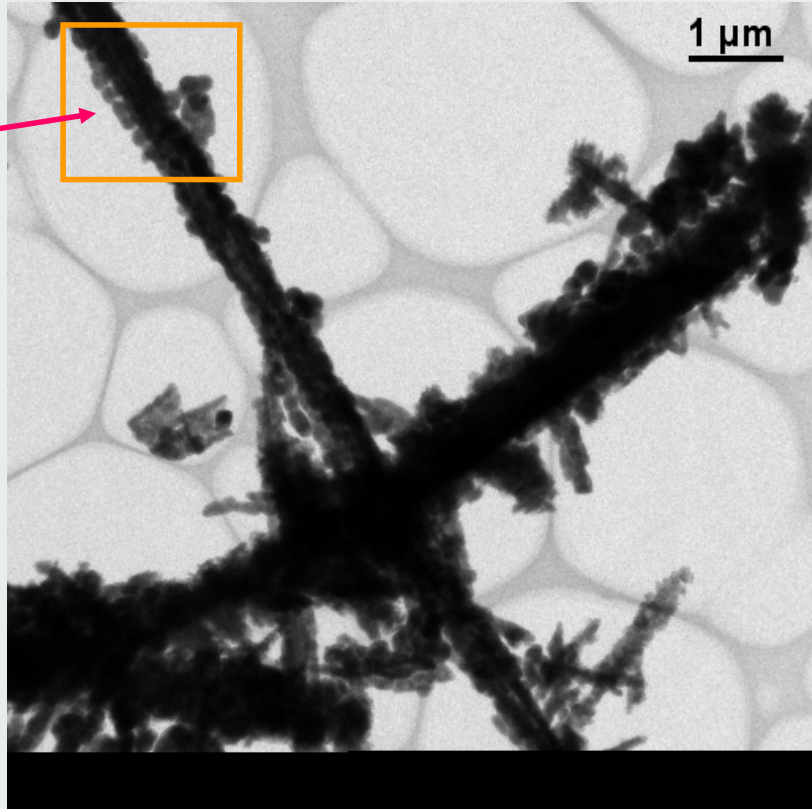
28

R. NESPER, ETH ZÜRICH & COLLEGIUM HELVETICUM



Surface Growth on Nanorods

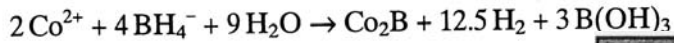
MnO₂
on
TiO₂



02.11.2006

Controlled Precursor Hydrolysis

Metal + Hydride Reaction



Magnetic Fluids: Fabrication, Magnetic Properties, and Organization of Nanocrystals**

By Marie-Paule Pileni*

Adv. Funct. Mater. **2001**, *11*, No. 5, October

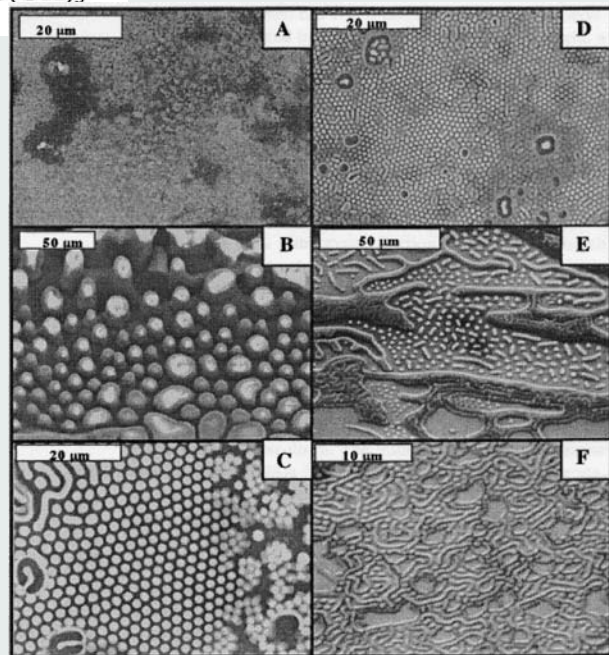


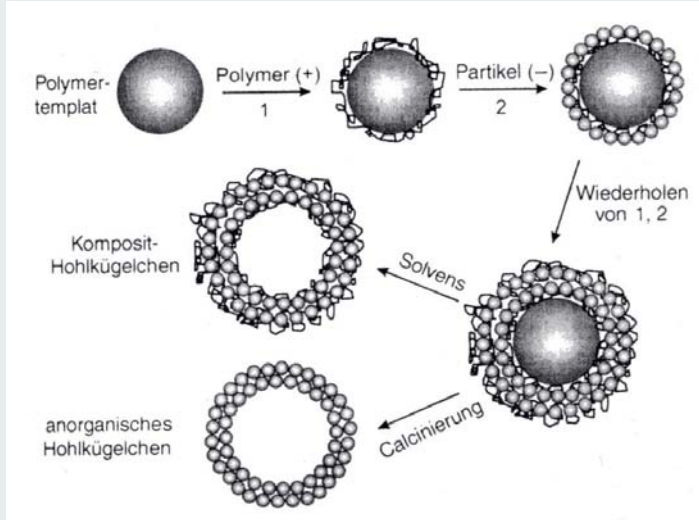
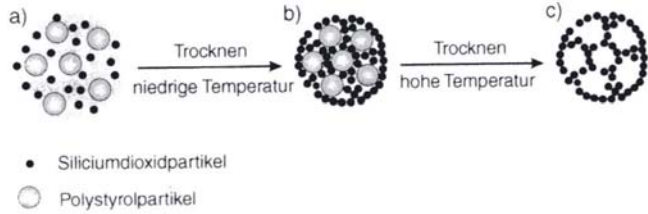
Fig. 14. SEM patterns obtained by evaporating 200 μL of a concentrated solution of cobalt nanocrystals (4×10^{-7} M in particles) deposited in a magnetic field perpendicular to the HOPG substrate. The evaporation time is 12 h. The strength of the applied field is 0 (A); 0.01 T (B); 0.27 T (C); 0.45 T (D); 0.60 T (E); and 0.78 T (F).

02.11.2006

Organische Template zur Formgebung anorganischer Materialien**

Kjeld J. C. van Bommel, Arianna Friggeri und Seiji Shinkai*

Adv. Funct. Mater. 2003, 13, No. 1, January



important route towards photonic crystals

02.11.2006

Nanochemistry UIO

31

Micelles/Vesicles as Nano Templates

Emergent Nanostructures: Water-Induced Mesoscale Transformation of Surfactant-Stabilized Amorphous Calcium Carbonate Nanoparticles in Reverse Microemulsions**

By Mei Li and Stephen Mann*

Nano Calcite
Bio Mineralization

Adv. Funct. Mater. 2002, 12, No. 11-12, I

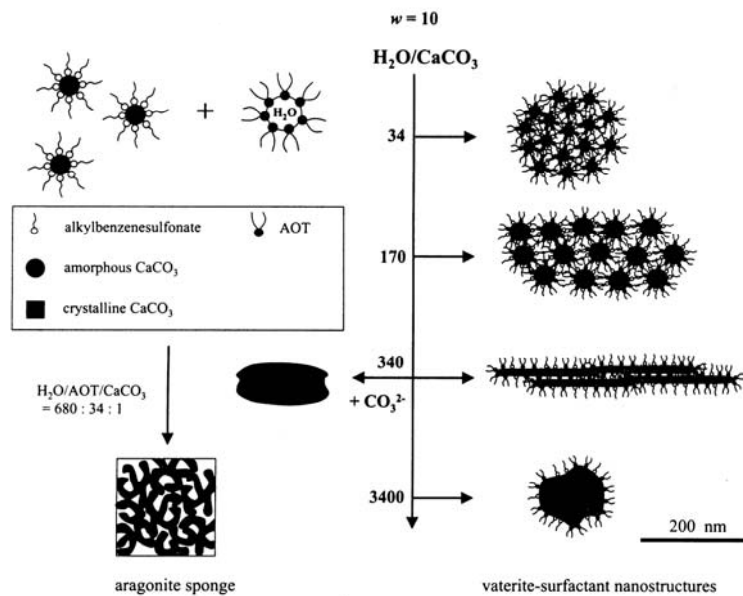


Fig. 8. General scheme showing experimental conditions and types of hybrid surfactant-vaterite nanostructures synthesized by microemulsion-mediated phase transformation of surfactant-stabilized ACC nanoparticles. Reactants are shown top/middle left. Nanostructures produced at $w = 10$ using different water droplet/amorphous CaCO_3 nanoparticle ratios are shown on the right. The aggregated structures are drawn approximately to scale (bar = 200 nm).

02.11.2006

Loaded Micelles and Dendrimers

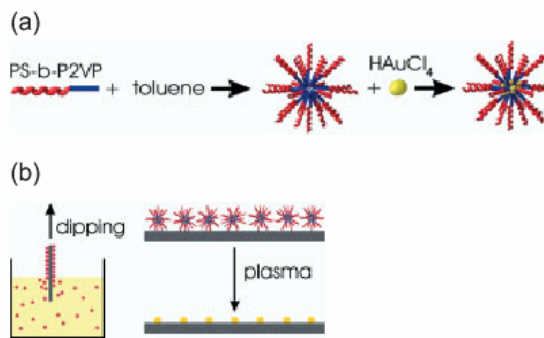


Fig. 1. a) Sketch of the formation of reverse micelles within PS-P2VP diblock copolymer solutions. The core of the micelle can be loaded with a metal precursor (e.g., HAuCl₄). b) The reverse micelles in solution are transferred onto substrates by dip coating. The polymer is removed and, simultaneously, the metal salt is reduced by applying either an oxygen plasma followed by a hydrogen plasma or by a single hydrogen plasma step (more details are given below).

02.11.2006

Nanochemistry UIO

33

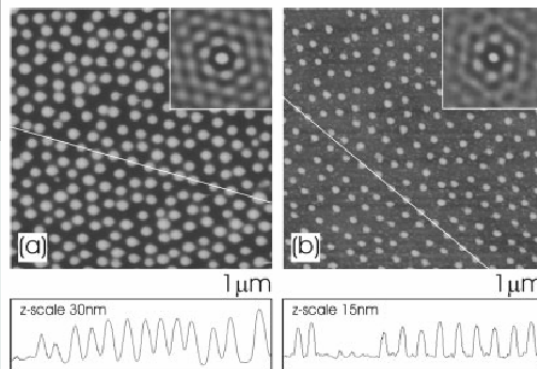


Fig. 2. Gold-loaded micelles on a silicon substrate before (a), z-scale 30 nm) and after (b), z-scale 15 nm) removal of the polymer matrix. Clearly, the order of the resulting nanoparticles reflects the order of the original micellar array. Local order is reasonably good as proven by the autocorrelation functions in the insets. The bottom panels show the results of line scans measured along the white lines shown.

Loaded Micelles and Dendrimers

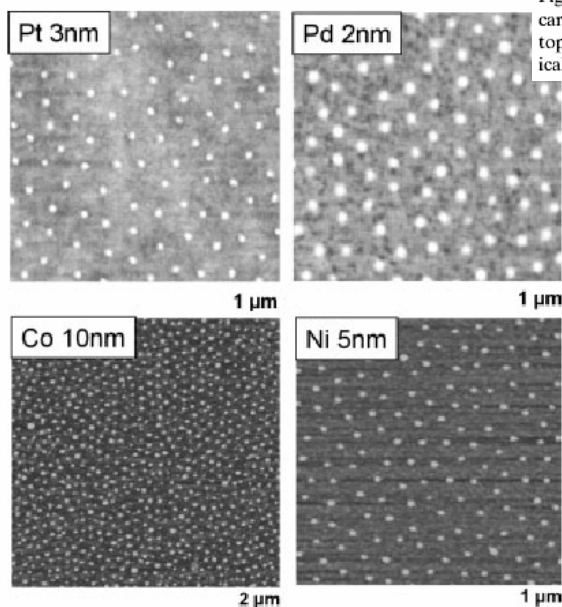


Fig. 11. AFM images of nanoparticles prepared from different elements. The universality of the micellar approach allows a wide variety of metallic, magnetic, or oxide particles to be prepared.

02.11.2006

Nanochemistry UIO

34

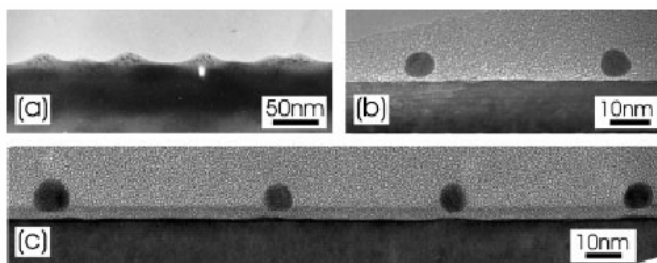
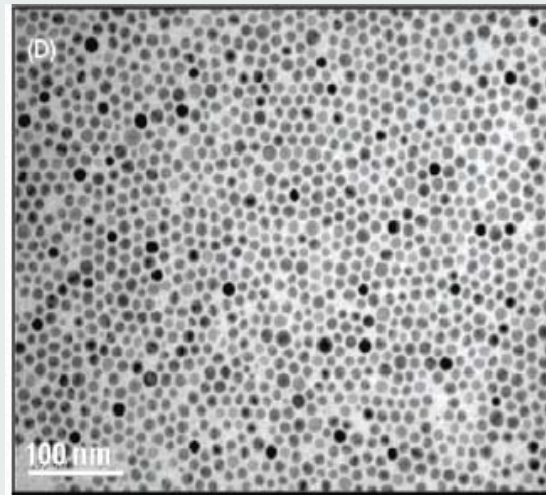
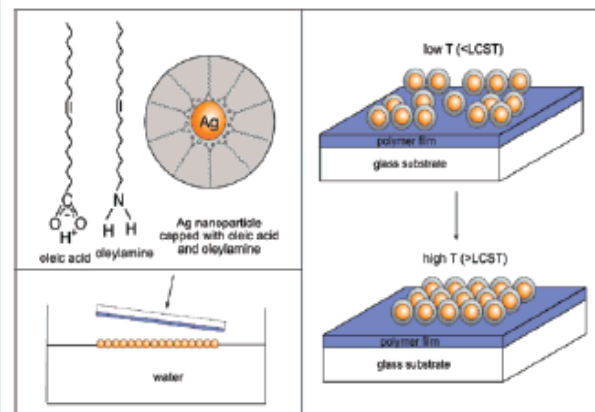


Fig. 10. TEM cross-section images of Au-salt-loaded micelles deposited onto a carbon-coated copper grid (a) and of the final array of Au nanodots prepared on top of a sapphire substrate (b) and on silicon (c), demonstrating the nearly spherical shape of the resulting particles.

Silver Nanospheres from Oleic Acid Emulsions



02.11.2006

Nanochemistry UIO

35

Nano Templates

Noble-Metal Nanotubes (Pt, Pd, Ag) from Lyotropic Mixed-Surfactant Liquid-Crystal Templates**

Tsuyoshi Kijima,* Takumi Yoshimura, Masafumi Uota, Takayuki Ikeda, Daisuke Fujikawa, Shinji Mouri, and Shinji Uoyama

Angew. Chem. 2004, 116, 230–234

Noble Metal Nano Tubes

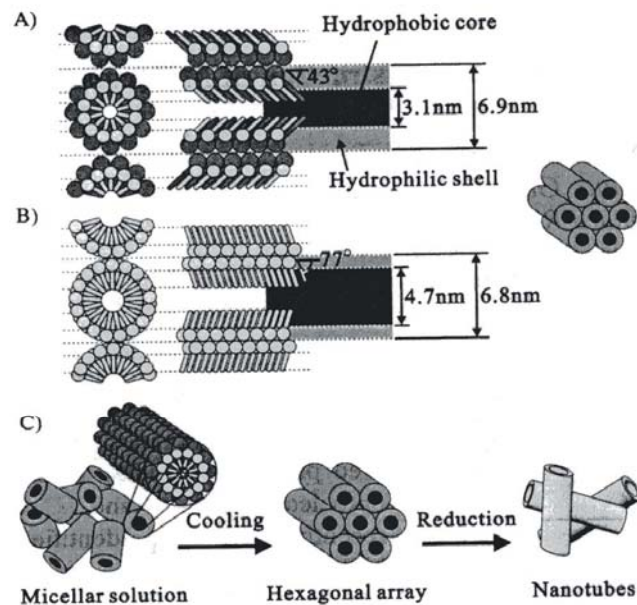
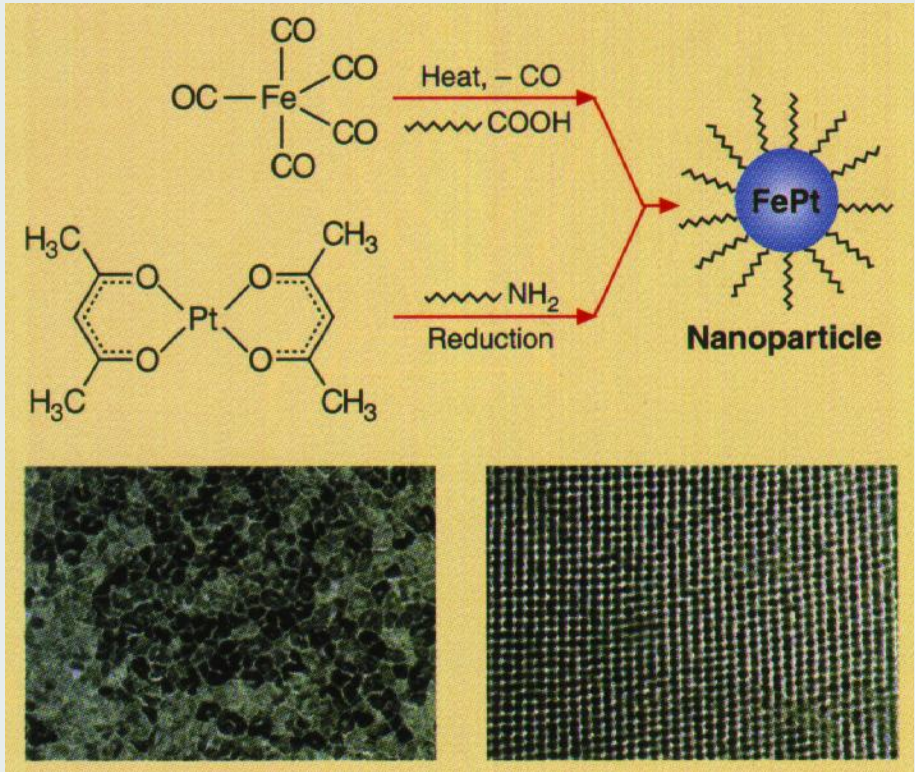


Figure 4. Schematic models for the formation of platinum nanotubes in the mixed surfactant templating system: A) Mixed ($C_{12}EO_9$ /Tween 60) and B) single ($C_{12}EO_9$) surfactant cylindrical rodlike micelles. C) Pathway from micellar solution to metal nanotubes by the reduction of metals salts confined to the aqueous shell of mixed-surfactant cylindrical micelles. The metal salts and water molecules are omitted from the models.

02.11.2006

Composite and Multimetallic Particles

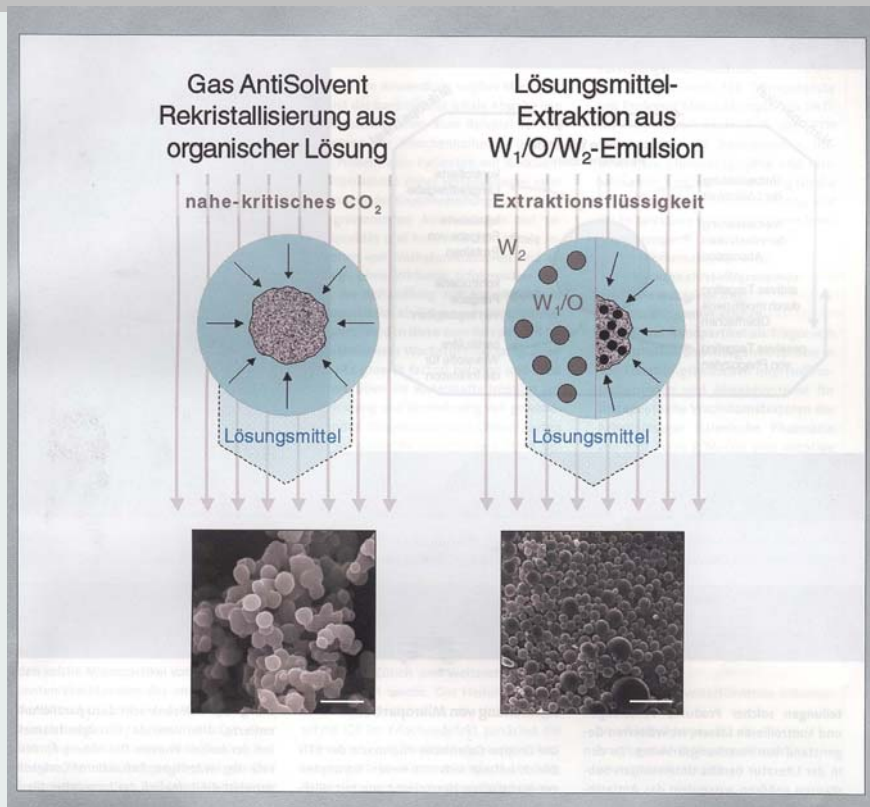


02.11.2006

Nanochemistry UIO

37

Extraction Methods



02.11.2006

Nanochemistry UIO

38

Spray Pyrolysis + Fly Ashes

An experimental and modeling investigation of particle production by spray pyrolysis using a laminar flow aerosol reactor

I. Wuled Lenggoro, Takeshi Hata, and Ferry Iskandar
 Department of Chemical Engineering, Hiroshima University, Kagamiyama 1-4-1,
 Higashi-Hiroshima 739-8527 Japan

Melissa M. Lunden
 Environmental Energy Technologies Division, Lawrence Berkeley National Laboratory,
 1 Cyclotron Road, Berkeley, California 94720

Kikuo Okuyama^{*)}
 Department of Chemical Engineering, Hiroshima University, Kagamiyama 1-4-1,
 Higashi-Hiroshima 739-8527 Japan

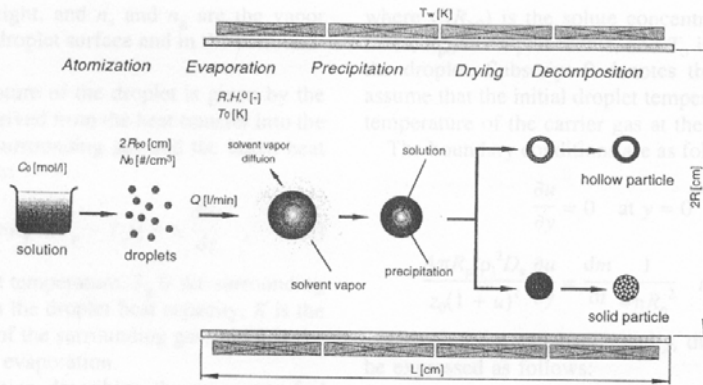


FIG. 3. Description of the simulation model.

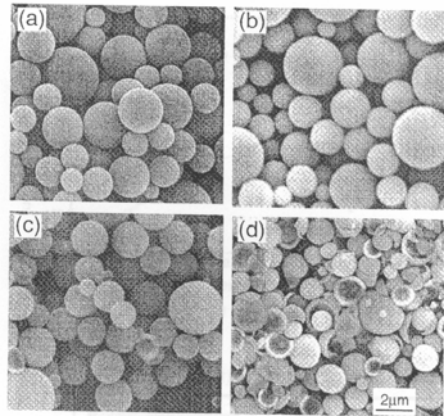
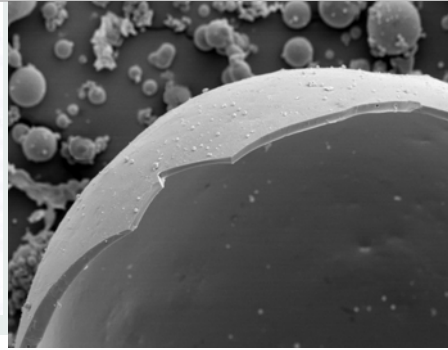


FIG. 6. Effect of furnace temperature on the morphology of zirconia particles: (a) 100 °C, (b) 200 °C, (c) 300 °C, and (d) 500 °C. Other experiment conditions: $C_0 = 2 \text{ mol/l}$; $Q = 2 \text{ l/min}$.

02.11.2006

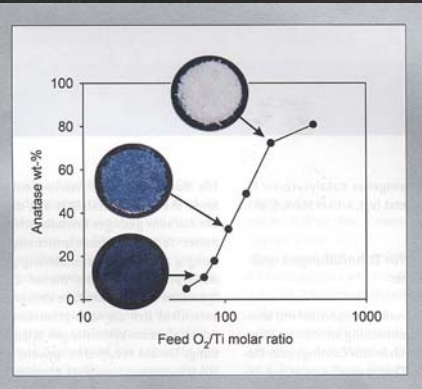
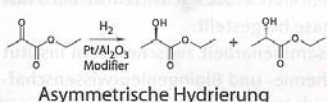
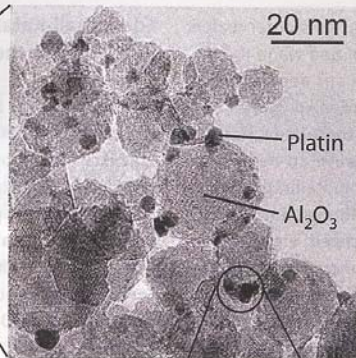
Nanochemistry UIO

Gas Phase Reactions

Flame Synthesis



Flammensynthese



02.11.2006

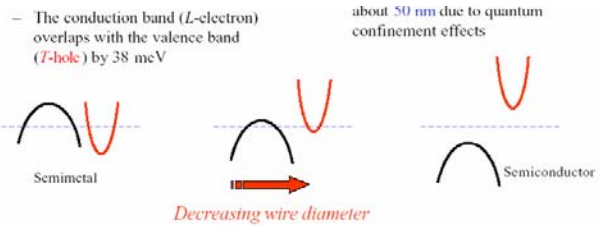
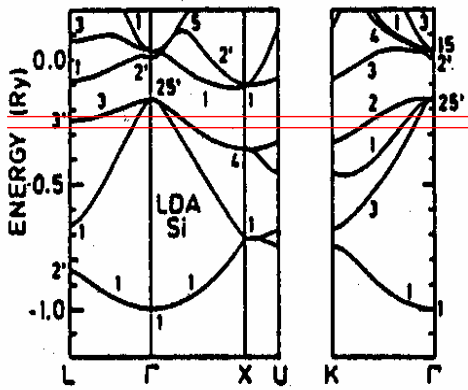
Nanochemistry UIO

Large industrial importance

40

Corrosion Methods and Phase Transitions

- | | |
|------------------------------|--|
| 1. Porous alumina | anodization |
| 2. Porous silicon | HF etching |
| 3. Porous metals evaporating | dealloying / etching / |
| 4. Amorphization of metals | reconstructive phase transitions,
hydriding/dehydr.
Precipitation (Raney metals) |



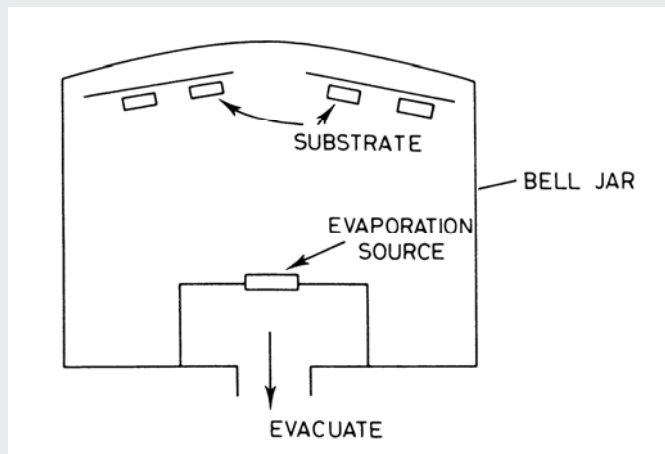
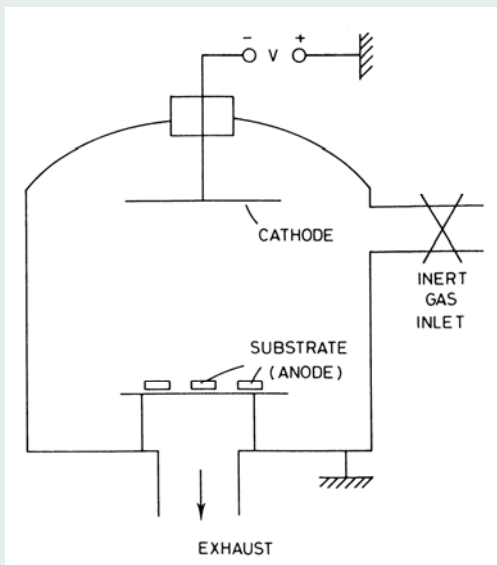
02.11.2006

Nanochemistry UIO

43

Thin films

Sputter technique

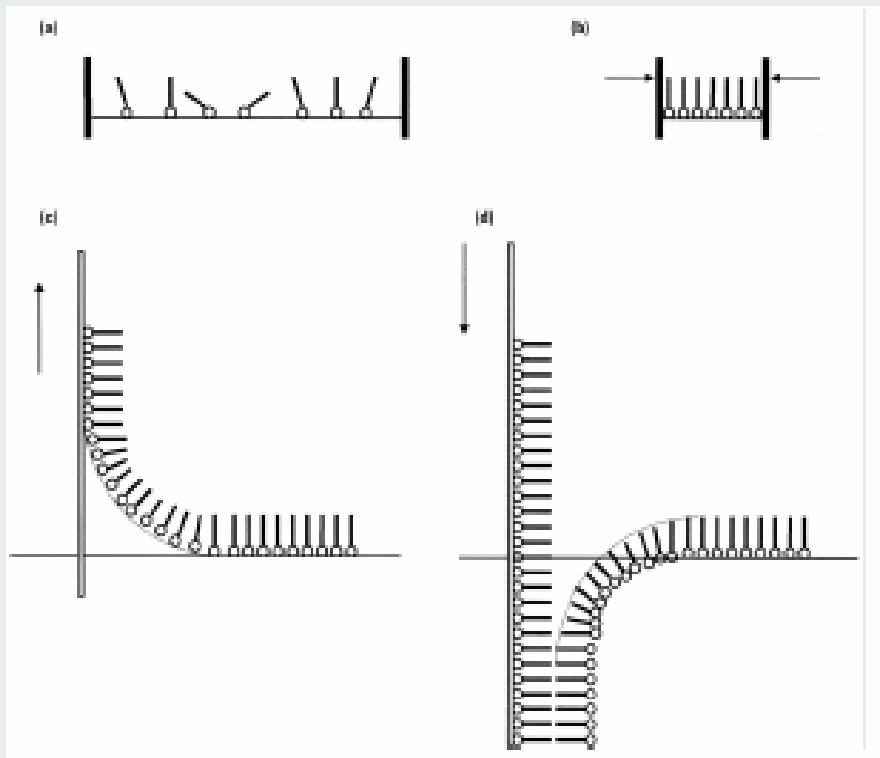


02.11.2006

Nanochemistry UIO

44

Langmuir Blodgett Films



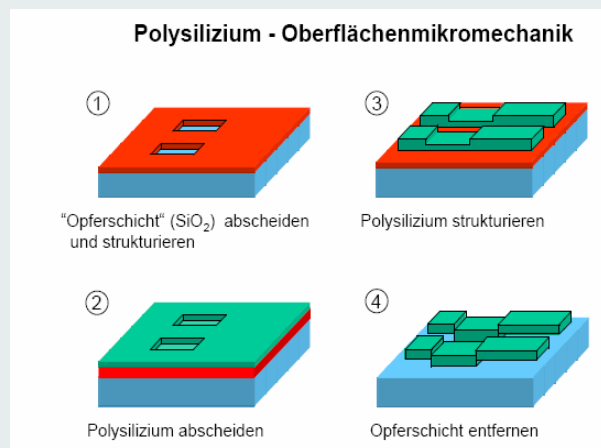
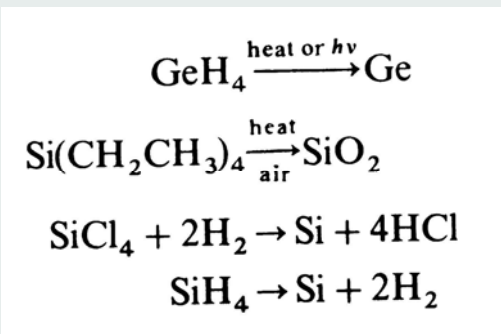
02.11.2006

Nanochemistry UIO

45

Thin Films

1. Chemical Vapor Deposition –CVD und MOCVD



TMA ---> Trimethylaluminium $\text{Al}(\text{CH}_3)_3$
 TMG ---> Trimethylgallium, $\text{Ga}(\text{CH}_3)_3$
 GaAs (3-5 - semiconductor) + PH_3 , AsH_3

02.11.2006

Nanochemistry UIO

46

1. Chemical Twinning
2. Double Salts of Zintl Phases
3. Layered Compounds
4. Intercalated Layered Compounds
5. Exfoliated Layered Compounds

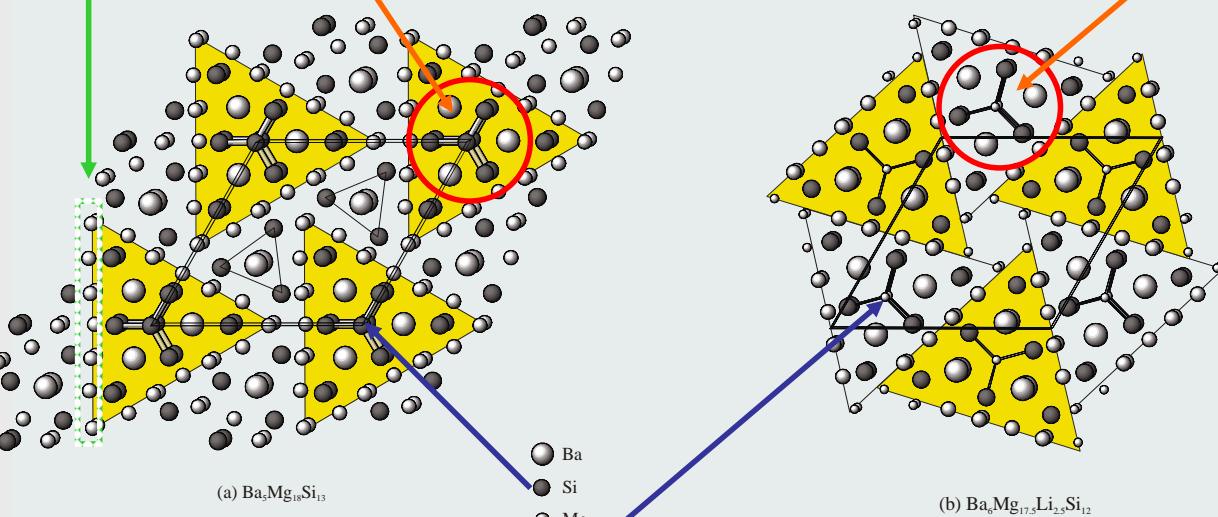
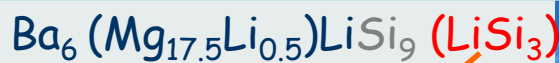
02.11.2006

Nanochemistry UIO

47

Direct Synthesis – Chemical Twinning - Intergrowth

S. Andersson; E. Parthe



02.11.2006

Nanochemistry UIO

48

Double Salts - Ordered Quantum Layers

R. NESPER ETH ZÜRICH & COLLEGIUM HELVETICUM

metallic

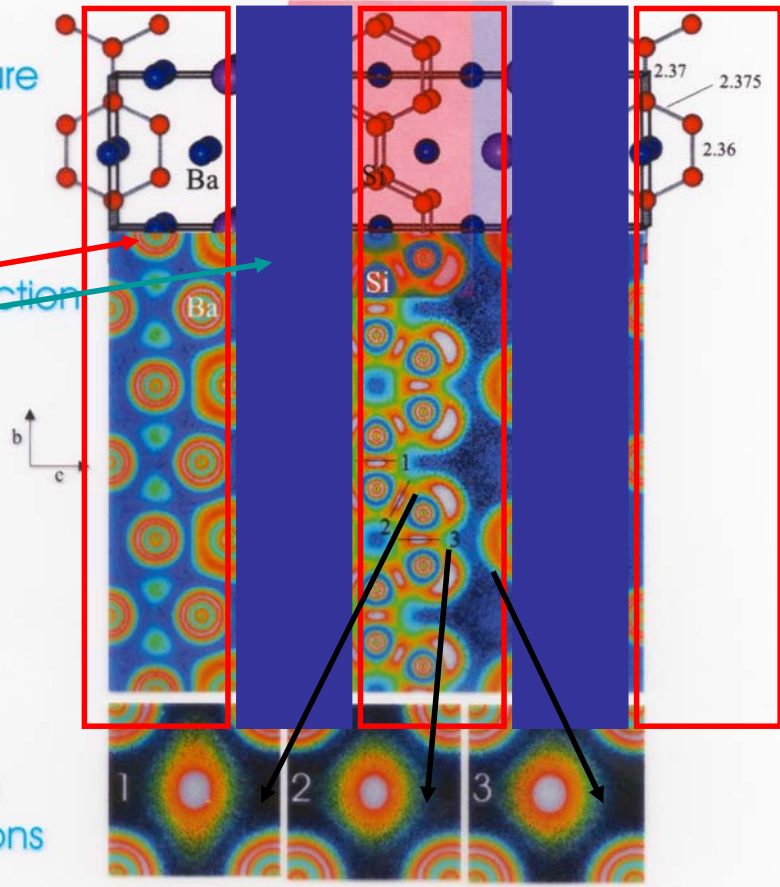
[Ba₂Si₃] [BaI₂]

insulating

Structure

ELF section

Elf
bond
sections



02.11.2006